Heliyon 10 (2024) e25458

Contents lists available at ScienceDirect

Heliyon

journal homepage: www.cell.com/heliyon

Research article

Equisetin inhibits adiposity through AMPK-dependent regulation of brown adipocyte differentiation

Qin Zhong [a,e,1], Xian Wang [a,1], Ruiran Wei [a,b], Fang Liu [a], Md Alamin [d], Jiajia Sun [c], Liming Gui [a,c,*,2]

[a] *Center for Tissue Engineering and Stem Cell Research, Guizhou Medical University, University Town, Gui'an New District, Guiyang City, Guizhou Province 550025, China*

[b] *Department of Basic Medical Sciences, Clinical College of Anhui Medical University, No.69 Meishan Road Hefei City, Anhui Province 230031, China*

[c] *Institute of Obstetrics and Gynecology, Shenzhen Peking University-Hong Kong University of Science and Technology Medical Center, No.1120 Lianhua Road, Futian District, Shenzhen City, Guangdong Province 518000, China*

[d] *Department of Biology, College of Life Sciences, Southern Medical University of Science and Technology, No.1088 Xueyuan Road, Shenzhen City, Guangdong Province 518055, China*

[e] *Clinical Medical Research Center, Affiliated Hospital of Guizhou Medical University No.28 Beijing Road, Guiyang City, Guizhou Province 550001, China*

ARTICLE INFO

Keywords:
Equisetin (EQST)
Adipogenesis
Lipogenesis
Brown adipocyte
Mitochondrial biogenesis
AMPK pathway

ABSTRACT

Obesity has a significant impact on endocrine function, which leads to metabolic diseases including diabetes, insulin resistance, and other complications associated with obesity. Development of effective and safe anti-obesity drugs is imperative and necessary. Equisetin (EQST), a tetramate-containing marine fungal product, was reported to inhibit bacterial fatty acid synthesis and affect mitochondrial metabolism. It is tempting to speculate that EQST might have anti-obesity effects. This study was designed to explore anti-obesity effects and underlying mechanism of EQST on 3T3-L1 adipocytes differentiated from 3T3-L1 cells. Oil Red O staining showed that EQST reduced lipid accumulation in 3T3-L1 adipocytes. Quantitative real-time polymerase chain reaction and Western blot analysis revealed that EQST significantly inhibited expression of adipogenesis/lipogenesis-related genes C/ebp-α, Ppar-γ, Srebp1c, Fas, and reduced protein levels. There was also increased expression of key genes and protein levels involved in lipolysis (Perilipin, Atgl, Hsl), brown adipocyte differentiation (Prdm16, Ucp1), mitochondrial biogenesis (Pgc1α, Tfam) and β-oxidation Acsl1, Cpt1. Moreover, mitochondrial content, their membrane potential ΔΨM, and respiratory chain genes Mt-Co1, Cox7a1, Cox8b, and Cox4 (and protein) exhibited marked increase in expression upon EQST treatment, along with increased protein levels. Importantly, EQST induced expression and activation of AMPK, which was compromised by the AMPK inhibitor dorsomorphin, leading to rescue of EQST-downregulated Fas expression and a reduction of the EQST-increased expression of Pgc1α, Ucp1, and Cox4. Together, EQST

* Corresponding author. Center for Tissue Engineering and Stem Cell Research, Guizhou Medical University, University town, Gui'an New District, Guiyang city, Guizhou Province 550025, China.

E-mail addresses: zhongqin@gmc.edu.cn (Q. Zhong), wangxian9586@163.com (X. Wang), 2453189440@qq.com (R. Wei), liufang70918@163.com (F. Liu), alamin@sustech.edu.cn (M. Alamin), arenalisa@163.com (J. Sun), dawnkwei@163.com (L. Gui).

[1] First author: Qin Zhong and Xian Wang contributed equally to this work.

[2] Present address: Dr Liming Gui: Institute of Obstetrics and Gynecology, Shenzhen Peking University-Hong Kong University of Science and Technology Medical Center, No.1120 Lianhua Road, Shenzhen City, Guangdong Province 518036, China.

https://doi.org/10.1016/j.heliyon.2024.e25458
Received 15 November 2023; Received in revised form 25 January 2024; Accepted 26 January 2024
Available online 1 February 2024

robustly promotes fat clearance through the AMPK pathway, these results supporting EQST as a strong candidate for the development into an anti-obesity therapeutic agent.

1. Introduction

Obesity and obesity-related metabolic disorders such as diabetes are a growing public health concern worldwide. The global prevalence of obesity has nearly tripled within the last 40 years [1]. The current treatments of anti-obesity have primarily focused on reducing energy intake. However, these measures were largely inefficient in maintaining long-term weight loss [2]. Therefore, developing effective and safe anti-obesity drugs is important and urgently needed [3].

Obesity is characterized by an increase in the number (hypertrophy) and size (hyperplasia) of adipocytes in adipose tissues [4,5]. Adipocytes arise from adipose tissue-derived mesenchymal stem cells (ADSCs). ADSCs develop into committed preadipocytes, which undergo growth arrest and initiate terminal differentiation into adipocytes when exposed to appropriate environmental cues [6–8]. There are three types of adipocytes: white adipocytes, classic brown adipocytes, and inducible brown adipocytes (also known as beige adipocytes) [9]. White adipocytes contain a single large lipid droplet, thus storing energy in the form of lipids and then breaking down stored lipids whenever energy is needed; whereas brown and beige adipocytes are both thermogenic adipocytes, characterized by multiple lipid droplets, large numbers of mitochondria and the ability to use energy to generate heat [9–11]. During adipose tissue development, a number of transcriptional factors and enzymes synergistically control distinct stages of lipid metabolism and enable adipocytes to maintain energy homeostasis. For example, CCAAT/enhancer-binding proteins (C/EBPs), peroxisome proliferator-activated receptor γ (PPAR-γ), sterol regulatory element-binding protein 1c (SREBP-1c) are involved in adipogenesis and fatty acid synthase (FAS) is associated with lipogenesis, including fatty acid synthesis and lipid accumulation [12]. Adipose TG lipase (ATGL), hormone-sensitive lipase (HSL) and perilipin (Plin), acyl-CoA synthase long-chain family member 1 (ACSL1) and carnitine palmitoyl transferase (CPT1) are separately related to lipolysis and fatty acid β-oxidation; PR domain containing 16 protein (PRDM16), tumor necrosis factor receptor superfamily member 9 (CD137), transmembrane protein 26 (TMEM26) and uncoupling protein 1 (UCP1), PPAR-γ coactivator (PGC1α) and mitochondrial transcription factor A (TFAM) are (inducible) brown adipocyte markers and regulate energy expenditure. These genes determine the adipocyte phenotype and function [8,9,13–18]. In addition, the adenosine 5′-monophosphate (AMP)-activated protein kinase (AMPK) acts as a sensor of cellular energy status and is involved in a multitude of developmental and functional processes of adipocytes [19]. Downregulation of AMPK has been found to increase lipogenesis and reduce fatty acid oxidation [20,21]. Any molecule that can inhibit excessive lipid accumulation in white adipocytes and/or promote energy expenditure via induction of brown adipocyte differentiation could be developed into an effective strategy to treat obesity and obesity-related comorbidities.

Equisetin (EQST), a tetramate-containing natural product with antibiotic and cytotoxic activity, was first derived from the terrestrial fungus Fusarium equisetin NRRL 5537 [22]. It was reported that equisetin inhibits bacterial acetyl-CoA carboxylase (ACC) in fatty acid synthesis and affects mitochondrial metabolism [21–24] suggesting that EQST has an important role in lipid metabolism.

3T3-L1 cells are a well-established preadipocyte cell line that was originally cloned from mouse Swiss 3T3 cells as a serial sub-strain expressing insulin receptors, with the potential to differentiate into mature adipocytes when treated with the MDI induction differentiation medium (0.5 mM 1-methyl-3-isobutylxanthine, 250 nM dexamethasone, and 160 nM insulin) [25]. 3T3-L1 cells are widely considered an ideal cellular model for identifying compounds that are involved in adipogenic differentiation and white adipocyte browning in the current study [26]. Here, we demonstrated that EQST significantly inhibits adipogenesis and lipogenesis, induces lipolysis and brown adipocyte differentiation accompanied by mitochondrial biogenesis to expend energy through the activation of the AMPK signaling pathway, and exhibits the potential for developing into an anti-obesity drug.

2. Materials and methods

2.1. Chemicals and reagents

Equisetin was purchased from Santa Cruz Biotechnology (Santa Cruz, CA, USA). Dulbecco's modified Eagle's medium, High glucose (DMEM/HG), fetal bovine serum (FBS), and penicillin–streptomycin solution (*P*–S) were purchased from Thermo Fisher Scientific (Waltham, MA, USA). Newborn calf serum (NBCS) was provided by Ausbian (Australia), 3-isobutyl-1-methylxanthine (IBMX, I5879), Rosiglitazone (RGZ, R2408), and dexamethasone (D4092) were obtained from Sigma-Aldrich (St. Louis, MO, USA), insulin from Solarbio (I8330, Beijing, China), Dimethyl sulfoxide (DMSO) and were supplied by Glentham Life Sciences (Corsham, UK). Antibodies against C/EBPα (#AF6333), PPAR-γ (#AF6284), SREBP1c (#AF6283), FAS (#ET-1701-91), PLIN (#DF7602), ATGL (#DF7756), HSL (#AF6403), ASCL1 (#DF9605), CPT1 (#DF12004), PRDM16 (#AF13303), UCP1 (#AFDF7720), PGC1α (#AF5395), TFAM (#AF0531), COX4 (#AF5468), AMP-activated protein kinase (AMPK; #AF6423), *anti*-phospho-AMPK (*p*-AMPK; #AF3423), and goat anti-rabbit IgG HRP (S0001) were provided by Affinity Biosciences (USA). All solvents, chemicals, and reagents were of analytical grade and purchased from Sigma-Aldrich, unless otherwise specified.

CCK-8 (SB792, Dojindo, Japan), MTT (M1020), Oil Red O stain kit (For Cultured Cells, G1262), Triglyceride (TG) assay kits (BC0625), Lactate dehydrogenase (LDH) activity detection kit (BC0685), Cell Cycle Analysis Kit (CA1510), Annexin V- Alexa Fluor 647/PI kit (CA1050), and Free Fatty Acid (FFA) content detection kit (BC0595) were purchased from Solarbio (Beijing, China). Mitotracker green (C1048) and Hoechst (33342) were provided by Beyotime Biotechnology (Beijing, China). Tetramethylrhodamine ethyl

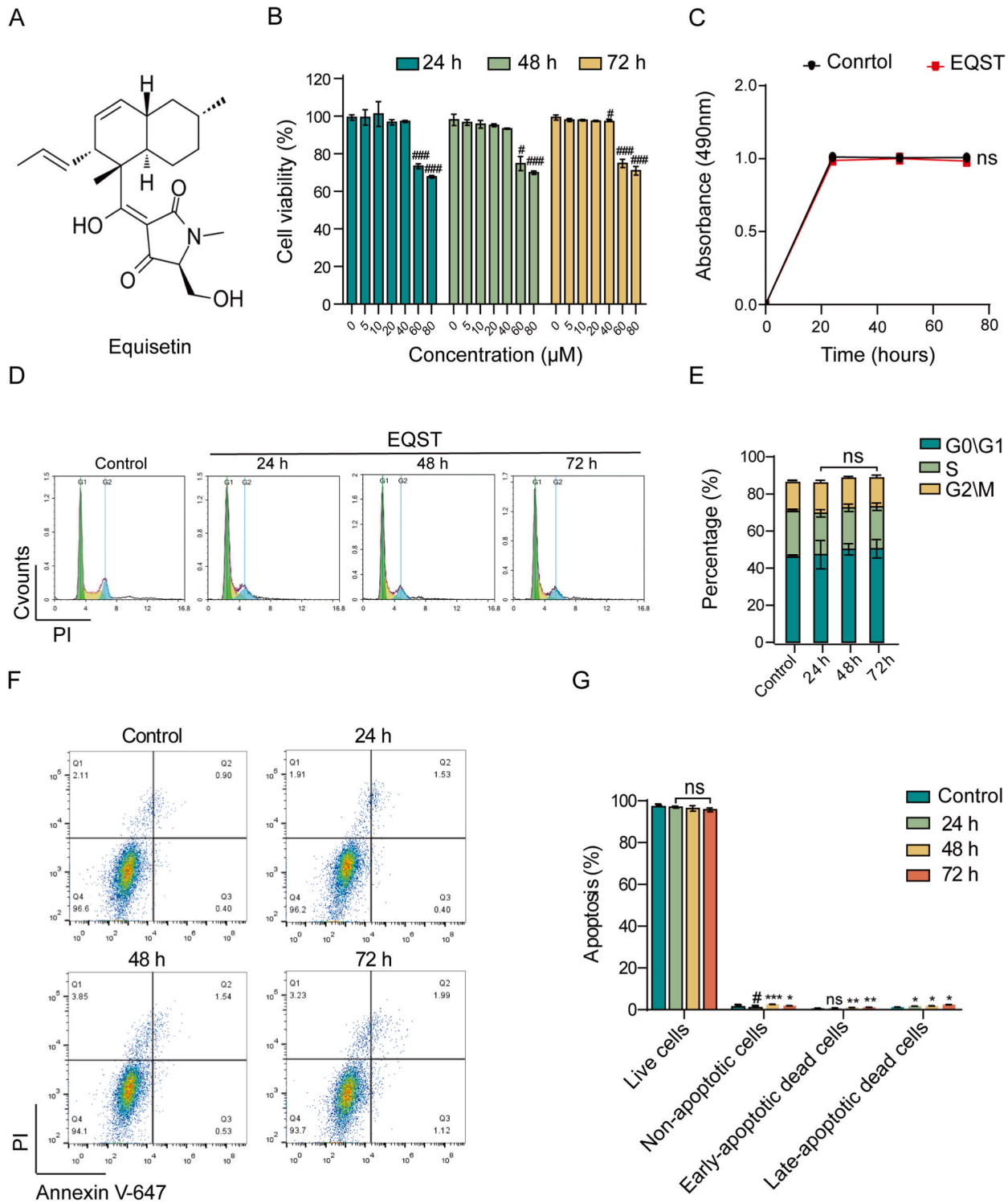

Fig. 1. The effect of EQST on 3T3-L1 cell viability for up to 72 h. (A) Chemical structure of EQST. **(B)** 3T3-L1 cell viability was measured by CCK8 assay after treatment with indicated concentrations of EQST range from 5 μM to 80 μM at 24h, 48h, 72 h. **(C)** 3T3-L1 cells were subjected for determining of cell growth using MTT assay, **(D** and **E)** cell cycle and **(F** and **G)** cell apoptosis through flow cytometry following treatment of 3T3-L1 cells with EQST for up to 72 h. Statistical analysis was carried out between EQST-treated group and control group. The data were presented as Mean ± standard error of the mean (SEM, $n = 3$). *increased compared to control, #: decreased compared to control. $^{*}p < 0.05$, $^{**}p < 0.01$, $^{***}p < 0.001$; $p < 0.001$, $\#\#p < 0.01$, $\#\#\#p < 0.001$.

ester perchlorate Kit (TMRE, HY-D0985A, Med Chem Express, USA), RNA-Quick Purification Kit (RN001), Fast All-in-One RT Kit (with gDNA Remover) (RT001), 2 × Super SYBR qPCR Master MIX (QP002) were obtained from ES Science (Shanghai, China), complete EDTA-free protease inhibitor (04693159001, Roche, Switzerland). All solvents, chemicals, and reagents were of analytical grade and purchased from Sigma-Aldrich, unless otherwise specified.

2.2. Cell culture

3T3-L1 cells were purchased from the Chinese Academy of Sciences Stem Cell Bank (SCSP-5038, Shanghai, China) and cultured in growth medium (GM) consisting of DMEM/HG medium supplemented with 10 % NBCS and 1 % penicillin-streptomycin at 37 °C with 5 % CO_2 in a humidified atmosphere.

2.3. Cell differentiation

To induce adipogenic differentiation, 3T3-L1 cells were seeded in 6-well plates (1×10^5 cells per well). At full confluence, 3T3-L1 cell differentiation (day 0) was induced in differentiation medium I (DM I) consisting of DMEM/HG medium supplemented with 10 % FBS, 1 % penicillin-streptomycin, 1 μg/mL insulin, 0.5 mM IBMX, 0.25 μM dexamethasone, and 2 μM rosiglitazone. 2 days later (day 2), DM I was withdrawn and switched to differentiation medium II (DM II), composing of DMEM/HG supplemented with 10 % FBS, 1 % penicillin-streptomycin and 1 μg/mL insulin. After 2 days (day 4) in DM II, 3T3-L1 cells were cultured in the maintenance medium without the addition of insulin until day 7. EQST was administered in the cultural medium from Day 0 until Day 7. To assess whether the AMPK signal pathway is involved in EQST-mediated fat metabolism, 3T3-L1 cells were treated with 5 μM AMPK inhibitor dorsomorphin (HY-13418A, Med Chem Express, USA) alone or with EQST. Untreated cells were used as a control. A schematic of the induced differentiation experiment is shown in Fig. 1C.

2.4. Cell viability assay

3T3-L1 cells were cultured in 96-well plates at 1×10^4 cells per well. At full confluence, 3T3-L1 cells were treated with DMSO or EQST at a concentration of 5 μM, 10 μM, 20 μM, 40 μM, 60 μM, 80 μM for 24 h, 48 h and 72 h. Cell viability was measured using Cell counting kit-8 and MTT cell proliferation and cytotoxicity assay kits and their absorbances were recorded at 450 nm and 490 nm, respectively using a plate reader (Bio-tek, USA). The experiments were performed according to the manufacturer's guidelines. Results were expressed as a percentage of viable cells relative to the control.

2.5. Cell cycle and apoptosis assay

3T3-L1 cells were cultured in 6-well plates at 1×10^5 cells per well. When fully confluent, DNA content quantitation assay (cell cycle) and Annexin V Alexa Fluor 647/PI assay kit were used to detect cell cycle and apoptosis in these cells, untreated or treated with 20 μM of EQST for 24 h, 48 h and 72 h, followed by quantification by flow cytometry (Beckman Coulter, USA). The data were further analyzed using Kaluza flowjo software. The percentage of cells in G0/G1, S, or G2/M phases and the apoptotic percentage were quantified relative to the control.

Apoptosis of the 3T3-L1 adipocytes at day 7 after the adipogenesis induction was assessed using a lactate dehydrogenase detection kit, followed by recording its absorbance at 450 nm using a microplate reader (Bio-tek, USA). All the experiments were done in triplicate according to the manufacturer's guidelines.

2.6. Oil red O staining and quantification

On Day 7 after the adipogenic induction differentiation, Oil Red O (ORO) staining was conducted to determine the lipid production using an ORO stain kit (For Cultured Cells) according to the manufacturer's instructions. Staining was visualized with an optical microscope (Nikon, Japan), and images were taken using an attached camera. To quantify lipid accumulation, the stained cells were dissolved in 100 % isopropanol and measured at 375 nm with a microplate reader (Bio-tek, USA).

2.7. Triglyceride measurement

For triglyceride assessment, the differentiated 3T3-L1 adipocytes at day 7 following the adipogenic induction were harvested, followed by determination of the content of the extracted triglycerides using a triglyceride detection kit, and its absorbance was measured at 420 nm using a microplate reader (Bio-tek, USA). The experiments were conducted according to the manufacturer's guidelines. The relative cellular triglyceride concentration was presented as a percentage of control.

2.8. Quantitative real-time PCR (RT-qPCR)

The total RNA was extracted using an RNA-Quick Purification Kit according to the manufacturer's instructions. RNA purity and concentration were measured using Nanodrop (Thermo Scientific, Wilmington, DE, USA). Full-length cDNAs were synthesized using a Fast All-in-One RT Kit (with gDNA Removel). All PCR was carried out using a Bio-Rad CFX96 real-time PCR system (Bio-Rad

Laboratories, USA) and gene expression was measured using SYBR-green and gene-specific primer sets. All primers were from BGI Biotechnology Co., Ltd. The sequences of the primers used in this study are listed in Table S1. The β-actin was used as a housekeeping gene. Target gene mRNA levels were normalized to β-actin using the $2^{-\Delta\Delta}$ Ct method.

2.9. Western blot analysis

The 3T3-L1 adipocytes in the presence and absence of EQST and/or AMPK inhibitor dorsomorphin (Dor) alone were washed with ice-cold PBS and then collected into a pre-cooled 1.5 mL Eppendorf tube. After centrifuging at 4 °C the resulting cell pellets were lysed in ice-cold RIPA buffer (Solarbio, Beijing, China), supplemented with 1 × cocktail inhibitors for 30 min, and then centrifuged at 4 °C. The supernatant was used as the whole cell lysate and kept at −80 °C until use. The protein concentration was determined using the Bradford assay. 30 μg protein of each sample were separated by 10 % sodium dodecyl sulfate-polyacrylamide gel electrophoresis (SDS-PAGE) (10 % TGX Stain-Free FastCast Acrylamide Kit (Bio-Rad, USA), transferred to polyvinylidene difluoride (PVDF) filter membranes (Immobilon-P, USA) and blotted with primary antibodies. The specific protein bands were visualized using enhanced chemiluminescent (ECL) detection reagents (Affinity Biosciences, USA), and detected by a Chemi Doc XRS + imaging system (Bio-Rad, USA). The intensity of each immunoreactive band was determined using the Image Lab Software Program.

2.10. Immunofluorescence staining assay

3T3-L1 adipocytes at day 7 following induction with or without EQST were fixed using 4 % (v/v) paraformaldehyde (Sigma-Aldrich), washed three times with PBS containing 0.1 % (v/v) Tween (PBST, Sigma-Aldrich) , and permeabilized using 0.1 % (v/v) TritonX-100 (Sigma-Aldrich) in PBS for 15 min at room temperature. After permeabilization, cells were blocked with 1 % BSA in PBST (PBSTB) for 30 min at room temperature and incubated with the primary antibody in PBSTB overnight at 4 °C. After the overnight incubation, cells were washed three times with PBST and stained with secondary antibodies fluorescence (FITC)-Conjugated affinipure goat anti-rabbit IgG (H + L) (Proteintech, SA00003-2, USA) diluted in PBST for 1 h at room temperature. The cells were washed three times in PBST and stained with DAPI (Solarbio, Beijing, China). The images were captured using a Leica fluorescence microscope, DMi8 (Leica Microsystems, Germany).

2.11. Measurement of free fatty acids

3T3-L1 cells were induced to differentiate in 6-well plates at 1×10^6 cells per well supplemented with or without 20 μM EQST up to 7 days. The cultural supernatant was collected to detect the amount of free fatty acid (FFA) released from the differentiated 3T3-L1 adipocytes at day 7 using a FFA content detection kit followed by measurement at 550 nm with the microplate reader (Bio-Tek, USA).

2.12. Mitochondrial content assay

The mitochondria of the differentiated 3T3-L1 adipocytes at day 7 after the adipogenic induction was detected using Mito-Tracker Green fluorescent mitochondrial stain. In order to determine mitochondrial content, 1×10^6 cells per well were seeded in 6-wells plates in the induction medium in the absence or presence of EQST. Mitochondria was labeled with a final concentration of dye of 1 μM for 30 min, then with nuclei co-stained using Hoechst 33342 nuclear staining at 37 °C for 10 min, followed by photography using a Leica fluorescence microscope DMi8 (Leica Microsystems, Germany). The fluorescence intensity was further measured using a microplate reader (Bio-Tek, USA) at 490 nm.

2.13. Mitochondrial membrane potential ($\Delta\psi M$) assay

Mitochondrial membrane potential (ΔΨM) was evaluated using the TMRE Kit. The 3T3-L1 adipocytes at day 7 after the induction differentiation were incubated with TMRE (1 μM) in fresh maintenance medium for 30 min and then with nuclei co-stained using Hoechst 33342 at 37 °C. By fluorescence microscopy, the signal intensity of TMRE fluorescence was observed and photographed using a Leica fluorescence microscope DMi8 (Leica Microsystems, Germany), followed by measurement with a microplate reader (Bio-Tek, USA) at 550 nm.

2.14. Statistical analysis

All data were presented as the mean ± standard error of the mean (SEM) of triplicates. The drug-treated and untreated cells were compared. Differences between mean values for control and samples for each group were analyzed using SPSS 13.0 software. The student's t-test was used for the evaluation of significance, and p values < 0.05 were regarded as a statistically significant difference. $p < 0.05$; $p < 0.01$; $p < 0.001$.

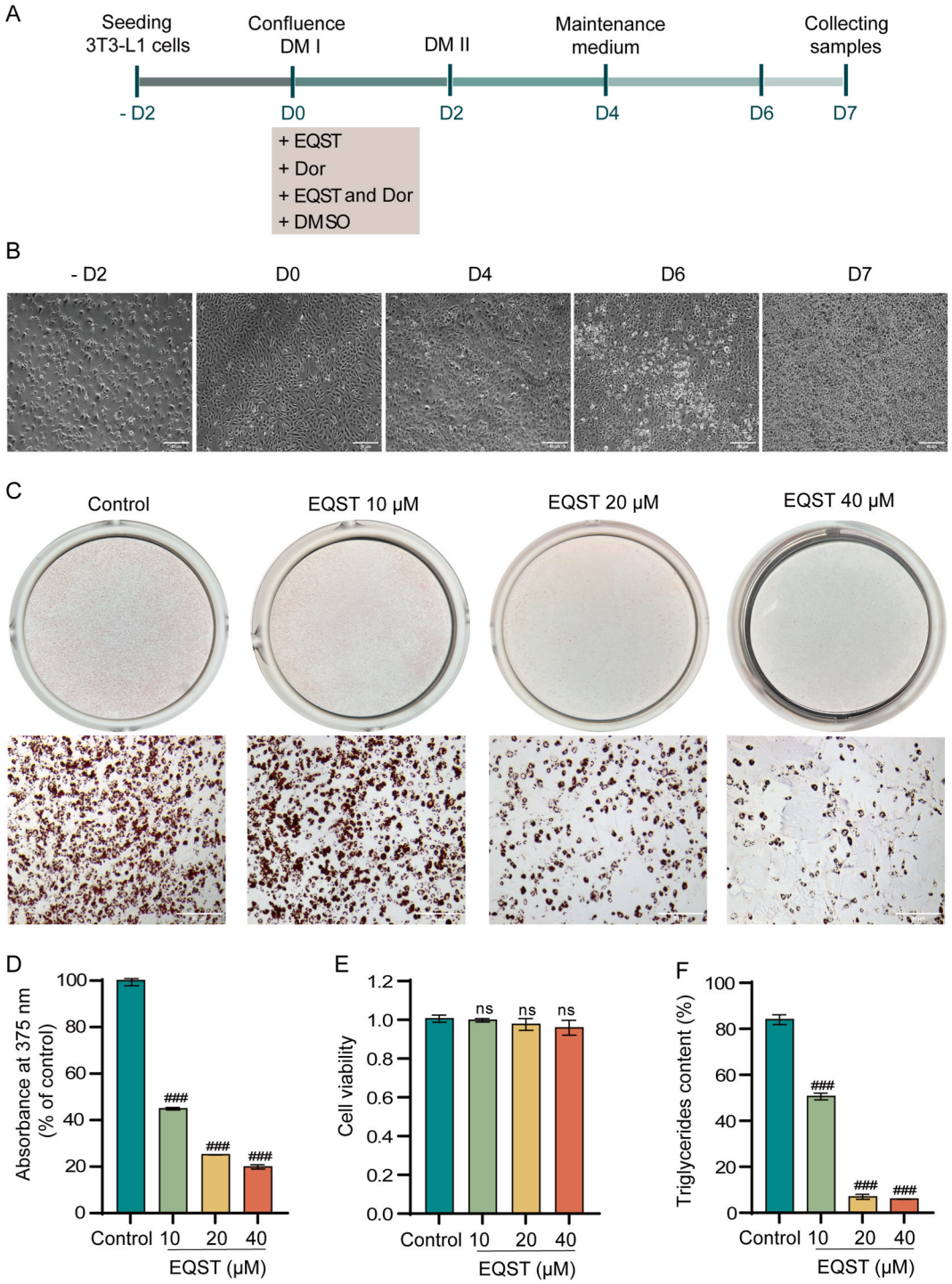

Fig. 2. EQST suppresses lipid accumulation without inducing apoptosis of 3T3-L1 adipocytes. (A) Strategies used for inducing adipogenic differentiation of 3T3-L1 cells in the presence or absence of EQST. **(B)** Lipid accumulation in the 3T3-L1 adipocytes were photographed under a Nikon optical microscope (magnification, × 20) following **(C)** ORO staining with nuclei co-stained with DAPI (blue) and **(D)** quantified by measuring absorbance at 375 nm. **(E)** Apoptotic percentage of the 3T3-L1 adipocytes treated with 20 μM EQST at day 7 after adipogenic induction differentiation by LDH release assay. **(F)** TG contents were detected using a triglyceride detection kit. The scale bar indicates 40 μm. Statistical analysis was carried out between EQST-treated group and control group. The data were presented as Mean ± standard error of the mean (SEM, n = 3). #: decreased compared to control. #p < 0.001, ##p < 0.01, ###p < 0.001. (For interpretation of the references to color in this figure legend, the reader is referred to the Web version of this article.)

3. Results

3.1. Effects of EQST on 3T3-L1 cell viability

EQST is a meroterpenoid containing tetramate (Fig. 1A). To explore the EQST mechanism of action on lipid metabolism, we set out to evaluate the effects of EQST on the viability of 3T3-L1 cells using a CCK8 assay. 3T3-L1 cells were cultured in the absence and/or presence of various concentrations of EQST ranging from 5 μM to 80 μM for 24 h, 48 h or 72 h. The data shows that 40 μM EQST did not significantly affect the viability of 3T3-L1 cells up to 72 h of culture, and the cell viability of the 3T3-L1 cells was higher than 90 % in the presence of 20 μM EQST for 72 h (Fig. 1B). Further, cell growth (Fig. 1C), cell cycle (Fig. 1D–E), and apoptosis analysis (Fig. 1F–G) by flow cytometry revealed that no significant difference was detected between the control and the 3T3-L1 cells treated with 20 μM EQST for up to 72 h. Thus, 20 μM EQST is safe for the viability of 3T3-L1 cells without causing cell growth inhibition or apoptosis.

3.2. EQST suppresses lipid accumulation without inducing apoptosis of 3T3-L1 adipocytes

Fig. 2A indicates a schematic of 3T3-L1 cell induction and differentiation. The 3T3-L1 cells were induced to differentiate into adipocytes (termed 3T3-L1 adipocytes) in the differentiation induction medium with different concentrations of EQST from 10 μM to 40 μM for 7 days. The Oil Red O (ORO) staining reveals that EQST dose-dependently suppressed lipid accumulation in the 3T3-L1 adipocytes (Fig. 2B). Of note, 20 μM EQST induced up to 75 % of fat clearance in the 3T3-L1 adipocytes at day 7 after the adipogenic differentiation (Fig. 2C). To rule out the reduction of lipid accumulation by EQST resulting from EQST-induced adipocyte apoptosis, the percentage of apoptotic 3T3-L1 adipocytes was tested by measuring lactate dehydrogenase (LDH) activity. As an indicator of adipocyte membrane integrity, this can be used as a measurement of viability (or apoptosis) [21]. The percentage cell viability of 3T3-L1 adipocytes remained higher than 95 % on day 7 after adipogenic induction in the presence of up to 40 μM EQST (Fig. 2D) compared to the control, suggesting that the lower concentrations than 40 μM EQST did not evidently induce apoptosis of the 3T3-L1 adipocytes while significantly suppressing lipid droplet accumulation. Colormetric analysis of intracellular triglyceride (TG) content shows decreased lipid accumulation with an increased dose of EQST, as indicated in the 3T3-L1 adipocytes (Fig. 2E). Taken together, these results show that EQST significantly inhibits lipid accumulation in vitro and 20 μM EQST is the optimal concentration for subsequent experiments.

3.3. EQST inhibits lipid accumulation by down-regulating expression of the key adipogenic and lipogenic genes and proteins

Adipogenic differentiation is accompanied by lipogenesis, which results in lipid accumulation. C/EBP-α and PPAR-γ are major transcriptional factors that are associated with adipogenic differentiation and increased expression of SREBP-1c. FAS is a late-stage differentiation marker for adipocytes [27]. SREBP-1c regulates the expression of FAS in the lipogenic pathway [28,29]. We assessed the impact of EQST on the expression of key adipogenic and lipogenic genes in the 3T3-L1 adipocytes on day 7 after adipogenic induction. The results show that EQST-treatment significantly downregulated the expression of C/ebp-α, Ppar-γ, Sbrep-1c, and Fas at both mRNA (Fig. 3A) and protein levels (Fig. 3B–C), compared to the controls (Fig. 3A). Implying that EQST reduced the lipid accumulation by suppressing the key adipogenic and lipogenic genes in the 3T3-L1 adipocytes.

3.4. EQST upregulates genes and proteins key to lipolysis and β-oxidation of fatty acids for adipose catabolism

By contrast, the promotion of lipolysis and fatty acid β-oxidation can reduce lipid accumulation. Perilipin coats the triglyceride

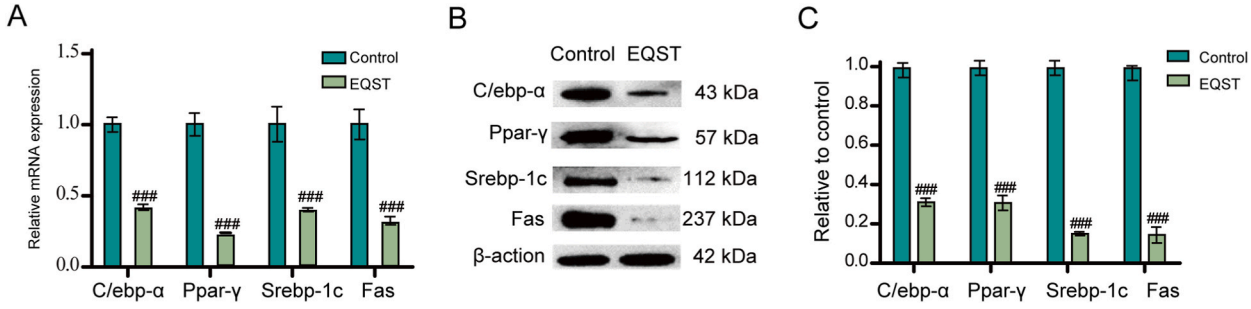

Fig. 3. EQST downregulates key adipogenic/lipogenic genes and proteins. 3T3-L1 cells were induced to differentiate with or without 20 μM EQST up to 7 days. (A) The mRNA levels of C/ebp-α, Ppar-γ, Sbrep-1c and Fas were measured by using quantitative real-time PCR. The target gene mRNA levels were normalized to β-actin using the $2^{-\Delta\Delta}$ Ct method. (B) The protein levels of C/ebp-α, Ppar-γ, Sbrep-1c and Fas were detected by the Western blotting and (C) The ratio of the intensity of specific bands of respective transcriptional factors from EQS T-treated groups against control after normalization to β-actin. The data were presented as Mean ± standard error of the mean (SEM, n = 3). Statistical analysis was carried out between EQST-treated group and the control group. *p < 0.05, **p < 0.01, ***p < 0.001; p < 0.001, ##p < 0.01, ###p < 0.001. *increased compared to control, #: decreased compared to control.

droplets and protects against lipolysis. ATGL and HSL are two key hydrolases within the lipolytic cascade and promote the formation of fatty acids (FAs) [30–33]. The produced FAs are specifically transferred into mitochondria for β-oxidation through ACSL1 and CPT1. On day 7 following adipogenic differentiation, EQST significantly upregulated the mRNA and protein expression of Plin1, Atgl, Hsl, Acsl1 and Cpt1 in the 3T3-L1 adipocytes (Fig. 4A–D). Further analysis of FA release into the culture medium revealed that a higher concentration of FAs was detected in the culture supplemented with EQST but not in the control (Fig. 4E). The findings suggest that EQST appears to activate lipolysis and stimulate fatty acid β-oxidation , which together contributed to fat clearance in the 3T3-L1 adipocytes.

3.5. EQST induces brown adipocyte differentiation and is accompanied by mitochondrial biogenesis

Lipolysis and β-oxidation are generally induced in brown adipocytes [34]. Preadipocytes can give rise to either white adipocytes or beige adipocytes. The results above prompted us to speculate that EQST could induce 3T3-L1 cell differentiation into brown adipocytes (BA) on day 7 after the induction differentiation. We therefore examined the expression of the specific BA markers Prdm16 and the uncoupling protein Ucp1, the mitochondrial markers Pgc1α, and Tfam. The results presented a significant markedly increased expression of these markers at both mRNA and protein levels in the EQST-treated cells compared to the control cells (Fig. 5A–C). IF staining further confirmed that increased expression of Prdm16 in the EQST-treated 3T3-L1 adipocytes in contrast to that in the control cells (Fig. 5D). In addition, we found that EQST upregulated mRNA expression of inducible brown adipocyte marker genes CD137 and Tmem 26 (Fig. 5A), which functionally relate to mitochondrial biogenesis. Meanwhile, the numbers of viable mitochondria in the 3T3-L1 adipocytes were measured using a mitochondrial green fluorescent probe. As shown in Fig. 5E, EQST treatment led to a marked increase in mitochondrial biogenesis compared to the control. Quantification of the fluorescence signals confirmed this result (Fig. 5F). These findings support the notion that EQST induced brown adipocyte differentiation accompanied by increased mitochondrial biogenesis.

The function of mitochondria in the 3T3-L1 adipocytes was further assessed by using the cationic fluorescent dye TMRE to monitor mitochondrial membrane potential ΔΨM [35]. A statistically significant increase of the mitochondrial ΔΨM in the 3T3-L1 adipocytes

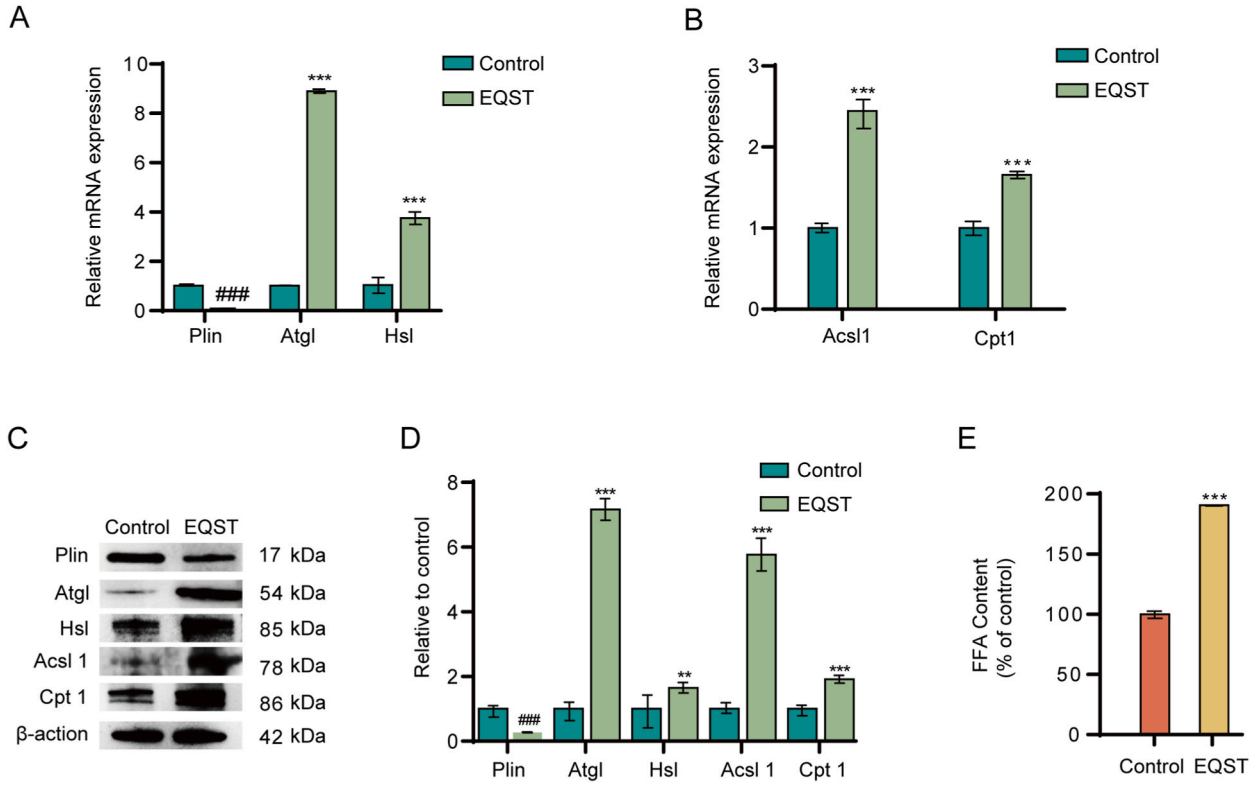

Fig. 4. EQST promotes lipolysis and subsequent fatty acid β-oxidation by upregulating expression of major lipolystic/oxidative genes and proteins. 3T3-L1 cells were induced to differentiate with or without 20 μM EQST up to 7 days. **(A)** The mRNA expression of lipolystic genes Atgl, Hsl and Plin1; **(B)** The mRNA expression of β-oxidation genes Acsl1 and Cpt1. The target gene mRNA levels were normalized to β-actin using the 2-ΔΔ Ct method. **(C)** The protein levels of, Atgl, Hsl, Plin1 and Acsl1 and Cpt1 were detected by the Western blotting and **(D)** The ratio of intensity of specific bands of different transcriptional factors from EQST-treated groups against control after normalization to β-actin. **(E)** The amounts of FAs released in the cultural medium was measured using FFA content detection kit. The data were presented as Mean ± standard error of the mean (SEM, $n = 3$). Statistical analysis was carried out between EQST-treated group and DMSO group. $^{*}p < 0.05$, $^{**}p < 0.01$, $^{***}p < 0.001$; $p < 0.001$, $\#\#p < 0.01$, $\#\#\#p < 0.001$.

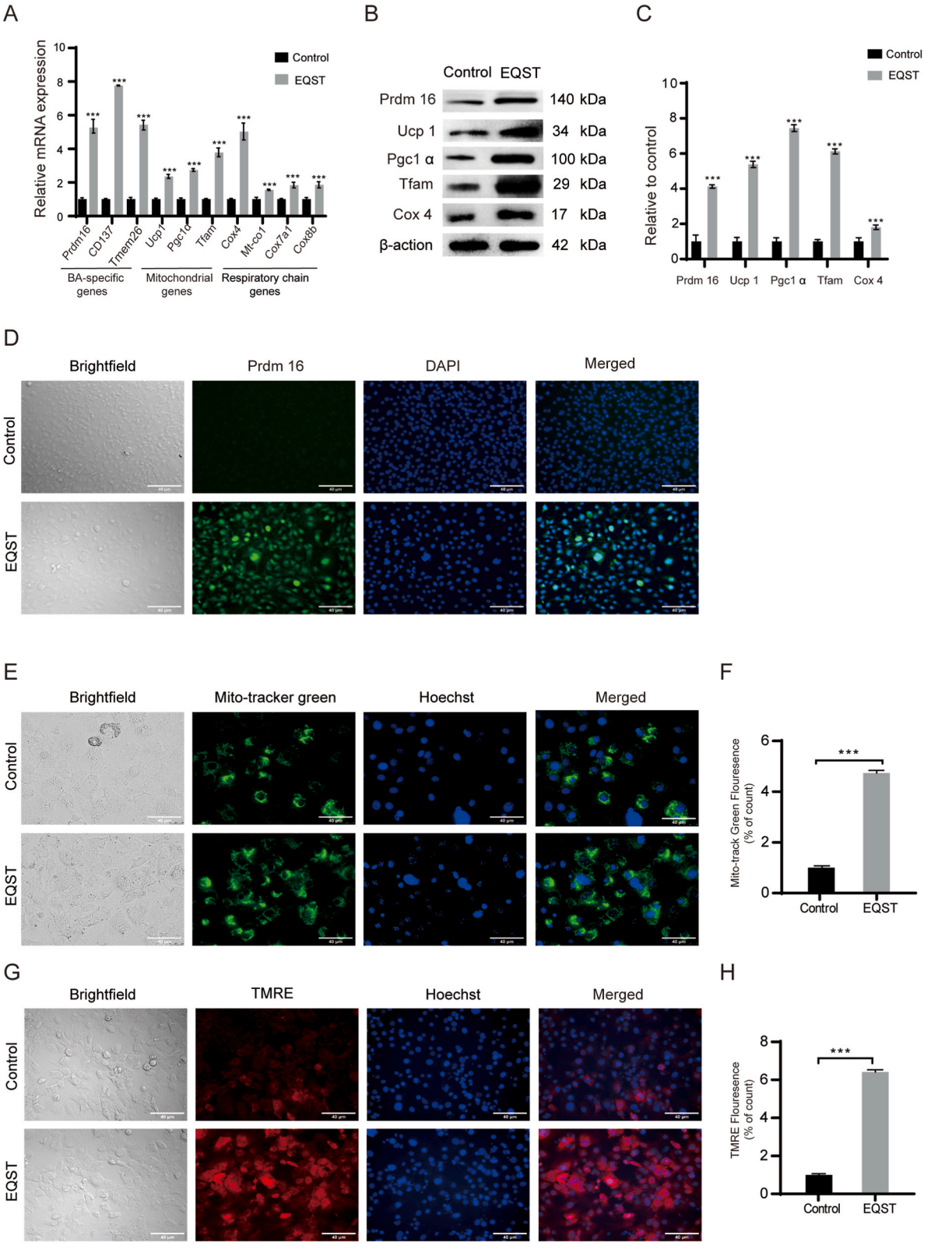

(caption on next page)

Fig. 5. EQST induces brown adipocyte differentiation and enhances mitochondrial performance by upregulating brown adipocyte-specific and mitochondrial genes and proteins. 3T3-L1 cells were induced to differentiate with or without 20 μM EQST up to 7 days. **(A)** The mRNA levels of BA-specific genes Prdm16, CD137, Tmem26, mitochondrial genes Ucp1, Pgc1α, Tfam and mitochondrial respiratory chain genes Mt-Co1, Cox7a1, Cox8b, and Cox4 were measured by Quantitative real-time PCR. **(B)** The protein levels of Prdm16, Ucp1, Pgc1α, Tfam, and Cox4 were detected by the Western blotting and **(C)** the ratio of the intensity of specific bands of different transcriptional factors from EQST-treated groups against control after normalization to β-actin was calculated. **(D)** Prdm16 protein expression (green) in the 3T3-L1 adipocytes by IF staining with nucleic-stained with DAPI (blue). **(E)** The mitochondria in living 3T3-L1 adipocytes were stained using mitochondrial green fluorescent probes with nuclei co-stained using Hoechst 33342 (blue). **(F)** The corresponding contents of mitochondria were detected at 495 nm with a microplate reader. **(Gg)** The mitochondrial membrane potential ΔΨM in the 3T3-L1 adipocytes was assessed using the cationic fluorescent dye TMRE () with nuclei co-stained with Hoechst 33342 (blue) and **(H)** the signal intensity of mitochondrial ΔΨM was detected at 495 nm using a microplate reader. All 3T3-L1 adipocytes stained were observed and analyzed using a fluorescence microscope (magnification, ×40). All target gene mRNA levels were normalized to β-actin using the 2-ΔΔ Ct method. The data were presented as mean ± standard error of the mean (SEM, n = 3). The scale bar indicates 40 μm. Statistical analysis was carried out between the EQST-treated group and the control group. ***$p < 0.001$. *: increased compared to control. (For interpretation of the references to color in this figure legend, the reader is referred to the Web version of this article.)

treated with EQST indicates that EQST-treatment enhanced mitochondrial function (Fig. 5G–H). Meanwhile, the mRNA expression of the mitochondrial respiratory chain genes Mt-Co1, Cox7a1, Cox8b, Cox4 (Fig. 5A), and Cox4 protein (Fig. 5B) was significantly higher in the EQST-treated 3T3-L1 adipocytes than that in the control cells, demonstrating that EQST enhances mitochondrial function. Taken together, our data demonstrate that EQST induces brown adipocyte differentiation from 3T3-L1 cells, and this process is accompanied by increased mitochondrial biogenesis and function.

3.6. EQST regulates lipid accumulation through the AMPK signal pathway

AMPK acts as a sensor of cellular energy status and is involved in various stages of lipid metabolism. We evaluated the action of EQST on the expression and phosphorylation of AMPK, and thus its activity. As shown in Fig. 6A–C, the mRNA and protein expression of AMPK along with the amount of phosphorylated AMPK (pAMPK) significantly increased after EQST treatment compared with the control, suggesting that EQST enhanced AMPK activity, and the AMPK pathway might be involved in the EQST-mediated fat metabolism. To confirm this hypothesis, we added dorsomorphin, a selective AMPK inhibitor at a dose of 5 μM to treat 3T3-L1 cells alone or with EQST during induction differentiation, followed by assessing the regulatory effects of EQST on the key factors related to lipid metabolism. The findings show that dorsomorphin blocked the phosphorylation of AMPK, which was partially recovered with EQST treatment compared to the group treated with dorsomorphin alone; consistently, dorsomorphin largely compromised the EQST-increased expression of Pgc1a, Ucp1 and Cox4 while slightly rescuing the downregulated expression of Fas by EQST at both mRNA (Fig. 6D) and protein levels (Figs. 6E and 5F). Meanwhile, ORO staining assays revealed that the reduced lipid accumulation by EQST was evidently restored by dorsomorphin (Fig. 6G and H). Altogether, the data suggested that the effect of EQST on fat clearance is mediated through activation of the AMPK signal pathway.

4. Discussion

It has previously been reported that EQST, a fungal natural compound, possesses antibiotic and cytotoxic activity by targeting bacterial fatty acid synthesis and mitochondrial metabolism [21–24]. However, limited information has been available regarding its effects on lipid metabolism at the cellular level in mammals. This study aimed to elucidate the effects of EQST on lipid metabolism and the underlying mechanism in vitro using 3T3-L1 preadipocytes as a cellular model. In the present study, analysis of EQST cytotoxicity suggests that 20 μM EQST reduced lipid accumulation in the 3T3-L1 adipocytes by 25 % without causing cell growth inhibition or apoptosis. Further investigation revealed that EQST treatment significantly downregulated the expression of key adipogenic/lipogenic genes C/EBPα, PPAR-γ, SBRBP-1c, and Fas in the 3T3-L1 adipocytes. It is well documented that during induction differentiation of 3T3-L1 preadipocytes, transient expression of C/EBPβ and C/EBPδ activates the beginning of the adipogenic process and upregulates the expression of PPAR-γ, C/EBPα, and SREBP-1c. The PPAR-γ and C/EBPα then cooperate with SREBP-1c to induce adipocyte differentiation and expression of a key lipogenic enzyme, FAS that promotes lipid accumulation in the form of triglycerides (TGs) [36–39]. In line with gene expression, we discovered that EQST dose-dependently reduced the content of triglycerides (TGs) in the 3T3-L1 adipocytes indicating that EQST suppresses lipid accumulation by downregulating key genes involved in adipogenesis/lipogenesis. These key factors may serve as drug targets to reduce excess fat.

Likewise, the lipolytic pathway to expend energy through thermogenesis in the brown adipocytes is an alternative pathway to reduce fat accumulation. In adipose tissue, Perilipin normally covers the triglyceride droplets within cells and blocks ATGL and HSL from gaining access to the droplets [18,31]. ATGL and HSL are two key hydrolases that account for more than 90 % of TG hydrolysis [40]. ATGL regulates the first step in TG hydrolysis, generating diglycerides (DG) and fatty acids, and HSL efficiently degrades DG, generating malonyl-CoA (MG) and FAs [32,41]. The fatty acids that are produced are released and then mobilized into mitochondria for fatty acid β-oxidation through ACSL1 and CPT-1 [30,32]. ACSL1 initiates the activation of FAs and catalyzes the formation of acyl-CoAs and specifically directs FAs towards mitochondrial β-oxidation [42]. Carnitine palmitoyl transferase (CPT1) promotes the transfer of long-chain fatty acyl CoA into mitochondria for β-oxidation [30]. The detection of released FAs collected from the culture medium exhibited a marked increase in the EQST-treated 3T3-L1 adipocytes. RT-qPCR and Western blotting analysis reveal that Plin, Atgl, Hsf1, CPT1 and ACSL1 were expressed significantly higher in the EQST-treated 3T3-L1 adipocytes, strongly suggesting that EQST

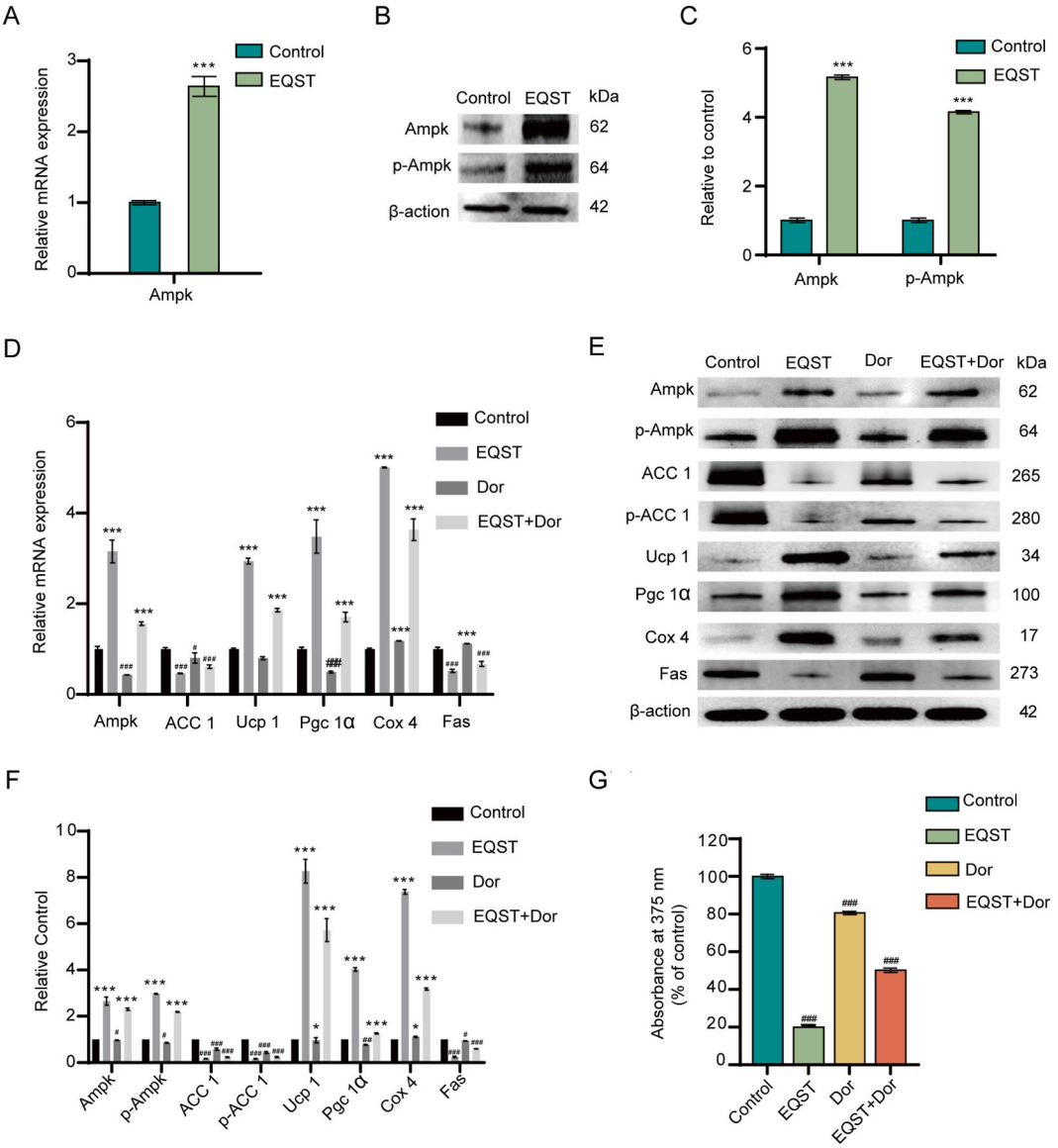

(caption on next page)

Fig. 6. EQST-mediated fat clearance depends on the AMPK signal pathway. (A) EQST treatment increased mRNA expression of AMPK. The 3T3-L1 adipocytes at day 7 following induction with or without 20 μM EQST and/or 5 μM Dor. **(B)** EQST stimulated protein expression and phosphorylation of AMPK, and **(C)** the ratio of the intensity of specific bands of different transcriptional factors from EQST-treated groups against control after normalization to β-actin. **(D)** Dorsomorphin, an AMPK inhibitor suppressed AMPK phosphorylation which was rescued by EQST. **(E)** Dorsomorphin largely reversed the increased expression of Pgc1α, Ucp1 and Cox4 by EQST while partially recovering the decreased expression of Fas enhanced by EQST at mRNA levels and **(F)** at protein levels. **(G)** The content of lipid droplets was analyzed using ORO staining with nuclei co-stained by DAPI (blue) and imaged using Nikon microscope (magnification, ×20) and **(H)** subsequent colorimetric assay at 375 nm following treatment with Dorsomorphin or EQST alone or combined Dorsomorphin and EQST. The target gene mRNA levels were normalized to β-actin using the 2-ΔΔ method. The data were presented as Mean ± standard error of the mean (SEM, n = 3). The scale bar indicates 40 μm. Statistical analysis was carried out between EQST-treated group and control group: ***$p < 0.001$; ###$p < 0.001$. *: increased compared to control; #: decreased compared to control. (For interpretation of the references to color in this figure legend, the reader is referred to the Web version of this article.)

contributes to fat clearance by enhancing lipolysis and subsequent fatty acid β-oxidation.

The lipid catabolic process mainly occurs in brown/beige adipocytes that differentiate from preadipocytes. PRDM16 is a master regulator of the cellular lineage that gives rise to brown adipocytes and (inducible) brown adipocytes [43]. PGC-1α is a master mitochondrial marker that particularly stimulates *de novo* mitochondrial biogenesis. PRDM16 and PGC1α synergistically induce brown adipocyte differentiation and mitochondrial biogenesis and enhance the expression of Ucp1 [44]. UCP1 expression is a unique feature of brown adipocytes and is generally accepted as the defining marker of brown adipocytes [45,46]. Brown adipocytes specifically contain a large number of mitochondria and utilize high mitochondrial UCP1 to uncouple respiration and dissipate chemical energy as heat, thereby promoting lipid consumption. Importantly, EQST significantly increased the mRNA and protein expression of the BA-specific markers Prdm16 and Ucp1 as well as mitochondrial markers Pgc1α, Tfam along with increased mitochondrial contents in the EQST-treated 3T3-L1 adipocytes. Of note, IF staining confirmed that Prdm16 was expressed at higher levels in the EQST-treated 3T3-L1 adipocytes. The mRNA expression of CD137 and TMEM26, which are beige adipocyte markers and are functionally associated with mitochondrial biogenesis, was also upregulated. Together, our data support the hypothesis that EQST induces brown adipocyte differentiation from 3T3-L1 preadipocytes and additionally stimulates mitochondrial biogenesis.

The thermogenic function of brown adipocytes is conferred by UCP1, and the thermogenic capacity of a given brown adipocyte depends on its mitochondrial content and activity. PGC1α activates the transcription of NRF1, which in turn regulates the transcription of TFAM [47]. TFAM translocate to the mitochondrial matrix and stimulates mitochondrial gene expression [26] that is required for enhancing the mitochondrial respiratory capacity, thereby promoting β-oxidation and energy expenditure. Consistently, our analysis exhibited a significantly upregulated expression of mitochondrial respiratory chain genes Mt-Co1, Cox7a1, Cox8b, and Cox4 (and protein) in the EQST-treated 3T3-L1 adipocytes, reflecting enhancement of mitochondrial function in EQST-induced brown adipocytes. In this regard, Cox 4 catalyzes the final step in the mitochondrial electron transfer chain and is thus one of the major regulation sites for oxidative phosphorylation. Meanwhile, analysis of mitochondrial ΔΨM in the living cells demonstrated that EQST treatment resulted in a marked increase of mitochondrial ΔΨM, indicating that the increased mitochondrial amount simultaneously exhibited an enhanced respiratory activity. Together, our data suggest that EQST-induced brown adipocyte differentiation is accompanied by increased mitochondrial respiratory capability. Actually, EQST endowed the differentiated brown adipocytes with enhanced respiratory performance, by which EQST reduces lipid accumulation by expending energy for heat production. The strategic induction of brown adipocyte differentiation has emerged as an exciting new therapeutic measure to combat obesity due to its functional role in energy expenditure through increasing thermogenesis.

It has been reported that several highly conserved signaling pathways, such as the PI3K/Akt, JAK/STAT, Wnt/β-catenin, mitogen-activated protein kinase (MAPK), and AMPK signaling cascades, are involved in fat metabolism [48,49]. In this regard, AMPK plays a central role in maintaining energy homeostasis as it controls the metabolic switch between anabolic/catabolic pathways. AMPK causes both short-term effects via direct phosphorylation of metabolic enzymes, and longer-term effects by modulating gene expression. Activation of AMPK by phosphorylation in differentiated adipocytes is tightly associated with the inhibition of fatty acid synthesis [50] and the stimulation of fatty acid β-oxidation. Our findings reveal that the inhibitory effect of dorsomorphin on AMPK activity was largely rescued by EQST. In parallel, the downregulation of the lipogenic marker Fas and the up-regulation of the mitochondrial markers Pgc1α, Ucp1 and the mitochondrial respiratory chain gene Cox4 were largely reversed by administration of dorsomorphin. These results demonstrated that EQST can enhance expression and activation of AMPK, through which EQST promoted browning of 3T3-L1 adipocytes while inhibiting adipogenesis in the 3T3-L1 adipocytes. Therefore, EQST-mediated lipid metabolism is AMPK-dependent, consistent with our observations, it was suggested that AMPK can activate brown adipocytes by inhibiting adipogenesis, maintaining mitochondrial homeostasis, and inducing browning within white adipose tissue. A number of AMPK-activating compounds have been reported so far: metformin, resveratrol, berberine, AICAR, and rosiglitazone [51,52]. However, to date, there has been limited success in developing these compounds into effective anti-obesity agents for clinical applications due to unacceptable side effects [53]. Studying new anti-obesity drugs that are based on natural products is currently more favored and imperatively needed, given that natural molecules might exhibit weaker side effects, higher bioactivity, and ease of availability [54–56]. Our findings provide a solid experimental basis for the anti-obesity effect of EQST, a natural fungal product. Planning *in vivo* experiments is necessary for determining the dosage and the method of EQST administration. In addition, it is required to analyze how EQST activates AMPK pathway in detail given the importance of AMPK in the regulation of whole-body energy balance.

In conclusion, this study demonstrates that EQST robustly reduces lipid accumulation by synergistically inhibiting adipose anabolic pathways while enhancing catabolic pathways through the activation of the AMPK signaling pathway. The novel mechanism of EQST action may lead to its application in the ongoing fight off obesity with the greatest therapeutic benefit.

Funding statement

This research was supported by the National Natural Science Foundation of China (No. U1812403-04) and Sanming Project of Medicine in Shenzhen (No. SZSM202011016).

Institutional review board statement

Not applicable.

Informed consent statement

Not applicable.

Data availability statement

All data presented this study are available from the corresponding author, upon reasonable request.

CRediT authorship contribution statement

Qin Zhong: Writing – review & editing, Methodology, Investigation. **Xian Wang:** Methodology, Investigation. **Ruiran Wei:** Writing – review & editing, Methodology, Investigation. **Fang Liu:** Methodology, Investigation. **Md Alamin:** Methodology. **Jiajia Sun:** Methodology. **Liming Gui:** Writing – review & editing, Writing – original draft, Methodology, Conceptualization.

Declaration of generative AI and AI-assisted technologies in the writing process

Not applicable.

Declaration of competing interest

The authors declare that they have no known competing financial interests or personal relationships that could have appeared to influence the work reported in this paper.

Acknowledgments

We thank for all members of and Gui laboratory for active discussion.

Appendix A. Supplementary data

Supplementary data to this article can be found online at https://doi.org/10.1016/j.heliyon.2024.e25458.

References

[1] M.A. Ambele, P. Dhanraj, R. Giles, M.S. Pepper, Adipogenesis, A complex interplay of multiple molecular determinants and pathways, Int. J. Mol. Sci. 21 (12) (2020).
[2] R.R. Wing, S. Phelan, Long-term weight loss maintenance, Am. J. Clin. Nutr. 82 (1 Suppl) (2005) 222S–225S.
[3] D.P. Guh, W. Zhang, N. Bansback, Z. Amarsi, C.L. Birmingham, A.H. Anis, The incidence of co-morbidities related to obesity and overweight: a systematic review and meta-analysis, BMC Publ. Health 9 (2009) 88.
[4] A.L. Ghaben, P.E. Scherer, Adipogenesis and metabolic health, Nat. Rev. Mol. Cell Biol. 20 (4) (2019) 242–258.
[5] A.G. Cristancho, M.A. Lazar, Forming functional fat: a growing understanding of adipocyte differentiation, Nat. Rev. Mol. Cell Biol. 12 (11) (2011) 722–734.
[6] T.J. Schulz, Y.H. Tseng, Brown adipose tissue: development, metabolism and beyond, Biochem. J. 453 (2) (2013) 167–178.
[7] M. Harms, P. Seale, Brown and beige fat: development, function and therapeutic potential, Nat Med 19 (10) (2013) 1252–1263.
[8] Y.H. Tseng, E. Kokkotou, T.J. Schulz, T.L. Huang, J.N. Winnay, C.M. Taniguchi, T.T. Tran, R. Suzuki, D.O. Espinoza, Y. Yamamoto, M.J. Ahrens, A.T. Dudley, A. W. Norris, R.N. Kulkarni, C.R. Kahn, New role of bone morphogenetic protein 7 in brown adipogenesis and energy expenditure, Nature 454 (7207) (2008) 1000–1004.
[9] J. Wu, P. Bostrom, L.M. Sparks, L. Ye, J.H. Choi, A.H. Giang, M. Khandekar, K.A. Virtanen, P. Nuutila, G. Schaart, K. Huang, H. Tu, W.D. van Marken Lichtenbelt, J. Hoeks, S. Enerback, P. Schrauwen, B.M. Spiegelman, Beige adipocytes are a distinct type of thermogenic fat cell in mouse and human, Cell 150 (2) (2012) 366–376.
[10] M.E. Lidell, M.J. Betz, O. Dahlqvist Leinhard, M. Heglind, L. Elander, M. Slawik, T. Mussack, D. Nilsson, T. Romu, P. Nuutila, K.A. Virtanen, F. Beuschlein, A. Persson, M. Borga, S. Enerback, Evidence for two types of brown adipose tissue in humans, Nat Med 19 (5) (2013) 631–634.
[11] L.Z. Sharp, K. Shinoda, H. Ohno, D.W. Scheel, E. Tomoda, L. Ruiz, H. Hu, L. Wang, Z. Pavlova, V. Gilsanz, S. Kajimura, Human BAT possesses molecular signatures that resemble beige/brite cells, PLoS One 7 (11) (2012) e49452.
[12] M. Lu, Y. Cao, J. Xiao, M. Song, C.T. Ho, Molecular mechanisms of the anti-obesity effect of bioactive ingredients in common spices: a review, Food Funct. 9 (9) (2018) 4569–4581.

[13] A. Matthias, K.B. Ohlson, J.M. Fredriksson, A. Jacobsson, J. Nedergaard, B. Cannon, Thermogenic responses in brown fat cells are fully UCP1-dependent. UCP2 or UCP3 do not substitute for UCP1 in adrenergically or fatty scid-induced thermogenesis, J. Biol. Chem. 275 (33) (2000) 25073–25081.
[14] T. Inagaki, J. Sakai, S. Kajimura, Transcriptional and epigenetic control of brown and beige adipose cell fate and function, Nat. Rev. Mol. Cell Biol. 17 (8) (2016) 480–495.
[15] W. Wang, P. Seale, Control of brown and beige fat development, Nat. Rev. Mol. Cell Biol. 17 (11) (2016) 691–702.
[16] G. Haemmerle, A. Lass, R. Zimmermann, G. Gorkiewicz, C. Meyer, J. Rozman, G. Heldmaier, R. Maier, C. Theussl, S. Eder, D. Kratky, E.F. Wagner, M. Klingenspor, G. Hoefler, R. Zechner, Defective lipolysis and altered energy metabolism in mice lacking adipose triglyceride lipase, Science 312 (5774) (2006) 734–737.
[17] J.S. Albert, L.M. Yerges-Armstrong, R.B. Horenstein, T.I. Pollin, U.T. Sreenivasan, S. Chai, W.S. Blaner, S. Snitker, J.R. O'Connell, D.W. Gong, R.J. Breyer 3rd, A. S. Ryan, J.C. McLenithan, A.R. Shuldiner, C. Sztalryd, C.M. Damcott, Null mutation in hormone-sensitive lipase gene and risk of type 2 diabetes, N. Engl. J. Med. 370 (24) (2014) 2307–2315.
[18] C. Sztalryd, D.L. Brasaemle, The perilipin family of lipid droplet proteins: gatekeepers of intracellular lipolysis, Biochim. Biophys. Acta Mol. Cell Biol. Lipids 1862 (10 Pt B) (2017) 1221–1232.
[19] D.G. Hardie, AMP-activated protein kinase: an energy sensor that regulates all aspects of cell function, Genes Dev. 25 (18) (2011) 1895–1908.
[20] C. Lee, J. Zeng, B.G. Drew, T. Sallam, A. Martin-Montalvo, J. Wan, S.J. Kim, H. Mehta, A.L. Hevener, R. de Cabo, P. Cohen, The mitochondrial-derived peptide MOTS-c promotes metabolic homeostasis and reduces obesity and insulin resistance, Cell Metabol. 21 (3) (2015) 443–454.
[21] M. Fernandez-Galilea, P. Perez-Matute, P.L. Prieto-Hontoria, M. Houssier, M.A. Burrell, D. Langin, J.A. Martinez, M.J. Moreno-Aliaga, alpha-Lipoic acid treatment increases mitochondrial biogenesis and promotes beige adipose features in subcutaneous adipocytes from overweight/obese subjects, Biochim. Biophys. Acta 1851 (3) (2015) 273–281.
[22] H.R. Burmeister, G.A. Bennett, R.F. Vesonder, C.W. Hesseltine, Antibiotic produced by Fusarium equiseti NRRL 5537, Antimicrob. Agents Chemother. 5 (6) (1974) 634–639.
[23] X. Liu, P.D. Fortin, C.T. Walsh, Andrimid producers encode an acetyl-CoA carboxyltransferase subunit resistant to the action of the antibiotic, Proc Natl Acad Sci U S A 105 (36) (2008) 13321–13326.
[24] E.C. Larson, A.L. Lim, C.D. Pond, M. Craft, M. Cavuzic, G.L. Waldrop, E.W. Schmidt, L.R. Barrows, Pyrrolocin C and equisetin inhibit bacterial acetyl-CoA carboxylase, PLoS One 15 (5) (2020) e0233485.
[25] H. Green, O. Kehinde, An established preadipose cell line and its differentiation in culture. II. Factors affecting the adipose conversion, Cell 5 (1) (1975) 19–27.
[26] B.L. Tang, Sirt1 and the mitochondria, Mol Cells 39 (2) (2016) 87–95.
[27] P.M. Ahmad, T.R. Russell, F. Ahmad, Increase in fatty acid synthetase content of 3T3-L cells undergoing spontaneous and chemically induced differentiation to adipocytes, Biochem. J. 182 (2) (1979) 509–514.
[28] S.R. Farmer, Transcriptional control of adipocyte formation, Cell Metabol. 4 (4) (2006) 263–273.
[29] E.D. Rosen, B.M. Spiegelman, What we talk about when we talk about fat, Cell 156 (1–2) (2014) 20–44.
[30] J.D. McGarry, N.F. Brown, The mitochondrial carnitine palmitoyltransferase system. From concept to molecular analysis, Eur. J. Biochem. 244 (1) (1997) 1–14.
[31] J. Martinez-Botas, J.B. Anderson, D. Tessier, A. Lapillonne, B.H. Chang, M.J. Quast, D. Gorenstein, K.H. Chen, L. Chan, Absence of perilipin results in leanness and reverses obesity in Lepr(db/db) mice, Nat. Genet. 26 (4) (2000) 474–479.
[32] R. Zimmermann, J.G. Strauss, G. Haemmerle, G. Schoiswohl, R. Birner-Gruenberger, M. Riederer, A. Lass, G. Neuberger, F. Eisenhaber, A. Hermetter, R. Zechner, Fat mobilization in adipose tissue is promoted by adipose triglyceride lipase, Science 306 (5700) (2004) 1383–1386.
[33] S. Fritah, E. Col, C. Boyault, J. Govin, K. Sadoul, S. Chiocca, E. Christians, S. Khochbin, C. Jolly, C. Vourc'h, Heat-shock factor 1 controls genome-wide acetylation in heat-shocked cells, Mol. Biol. Cell 20 (23) (2009) 4976–4984.
[34] J. Nedergaard, O. Lindberg, Norepinephrine-stimulated fatty-acid release and oxygen consumption in isolated hamster brown-fat cells. Influence of buffers, albumin, insulin and mitochondrial inhibitors, Eur. J. Biochem. 95 (1) (1979) 139–145.
[35] V. Bantseev, J.G. Sivak, Confocal laser scanning microscopy imaging of dynamic TMRE movement in the mitochondria of epithelial and superficial cortical fiber cells of bovine lenses, Mol. Vis. 11 (2005) 518–523.
[36] S. Mandrup, M.D. Lane, Regulating adipogenesis, J. Biol. Chem. 272 (9) (1997) 5367–5370.
[37] B. Huang, H.D. Yuan, D.Y. Kim, H.Y. Quan, S.H. Chung, Cinnamaldehyde prevents adipocyte differentiation and adipogenesis via regulation of peroxisome proliferator-activated receptor-gamma (PPARgamma) and AMP-activated protein kinase (AMPK) pathways, J. Agric. Food Chem. 59 (8) (2011) 3666–3673.
[38] T. Tanaka, N. Yoshida, T. Kishimoto, S. Akira, Defective adipocyte differentiation in mice lacking the C/EBPbeta and/or C/EBPdelta gene, EMBO J. 16 (24) (1997) 7432–7443.
[39] T.F. Osborne, Sterol regulatory element-binding proteins (SREBPs): key regulators of nutritional homeostasis and insulin action, J. Biol. Chem. 275 (42) (2000) 32379–32382.
[40] M. Schweiger, R. Schreiber, G. Haemmerle, A. Lass, C. Fledelius, P. Jacobsen, H. Tornqvist, R. Zechner, R. Zimmermann, Adipose triglyceride lipase and hormone-sensitive lipase are the major enzymes in adipose tissue triacylglycerol catabolism, J. Biol. Chem. 281 (52) (2006) 40236–40241.
[41] E. Smirnova, E.B. Goldberg, K.S. Makarova, L. Lin, W.J. Brown, C.L. Jackson, ATGL has a key role in lipid droplet/adiposome degradation in mammalian cells, EMBO Rep. 7 (1) (2006) 106–113.
[42] J.M. Ellis, L.O. Li, P.C. Wu, T.R. Koves, O. Ilkayeva, R.D. Stevens, S.M. Watkins, D.M. Muoio, R.A. Coleman, Adipose acyl-CoA synthetase-1 directs fatty acids toward beta-oxidation and is required for cold thermogenesis, Cell Metabol. 12 (1) (2010) 53–64.
[43] P. Seale, B. Bjork, W. Yang, S. Kajimura, S. Chin, S. Kuang, A. Scime, S. Devarakonda, H.M. Conroe, H. Erdjument-Bromage, P. Tempst, M.A. Rudnicki, D. R. Beier, B.M. Spiegelman, PRDM16 controls a brown fat/skeletal muscle switch, Nature 454 (7207) (2008) 961–967.
[44] T.B. Walden, I.R. Hansen, J.A. Timmons, B. Cannon, J. Nedergaard, Recruited vs. nonrecruited molecular signatures of brown, "brite," and white adipose tissues, Am. J. Physiol. Endocrinol. Metab. 302 (1) (2012) E19–E31.
[45] S.P. Commins, P.M. Watson, M.A. Padgett, A. Dudley, G. Argyropoulos, T.W. Gettys, Induction of uncoupling protein expression in brown and white adipose tissue by leptin, Endocrinology 140 (1) (1999) 292–300.
[46] R.A. Koza, S.M. Hohmann, C. Guerra, M. Rossmeisl, L.P. Kozak, Synergistic gene interactions control the induction of the mitochondrial uncoupling protein (Ucp1) gene in white fat tissue, J. Biol. Chem. 275 (44) (2000) 34486–34492.
[47] Z. Chen, S. Tao, X. Li, Q. Yao, Resistin destroys mitochondrial biogenesis by inhibiting the PGC-1 alpha/NRF1/TFAM signaling pathway, Biochem. Biophys. Res. Commun. 504 (1) (2018) 13–18.
[48] D. Wang, Y. Zhou, W. Lei, K. Zhang, J. Shi, Y. Hu, G. Shu, J. Song, Signal transducer and activator of transcription 3 (STAT3) regulates adipocyte differentiation via peroxisome-proliferator-activated receptor gamma (PPARgamma), Biol Cell 102 (1) (2009) 1–12.
[49] A. Guru, P.K. Issac, M. Velayutham, N.T. Saraswathi, A. Arshad, J. Arockiaraj, Molecular mechanism of down-regulating adipogenic transcription factors in 3T3-L1 adipocyte cells by bioactive anti-adipogenic compounds, Mol. Biol. Rep. 48 (1) (2021) 743–761.
[50] D.G. Hardie, F.A. Ross, S.A. Hawley, AMPK: a nutrient and energy sensor that maintains energy homeostasis, Nat. Rev. Mol. Cell Biol. 13 (4) (2012) 251–262.
[51] D. Garcia, R.J. Shaw, AMPK: mechanisms of cellular energy sensing and restoration of metabolic balance, Mol Cell 66 (6) (2017) 789–800.
[52] F.A. Duca, C.D. Cote, B.A. Rasmussen, M. Zadeh-Tahmasebi, G.A. Rutter, B.M. Filippi, T.K. Lam, Metformin activates a duodenal Ampk-dependent pathway to lower hepatic glucose production in rats, Nat Med 21 (5) (2015) 506–511.
[53] S. Colagiuri, Diabesity: therapeutic options, Diabetes Obes. Metabol. 12 (6) (2010) 463–473.

[54] T.D. Muller, C. Clemmensen, B. Finan, R.D. DiMarchi, M.H. Tschop, Anti-obesity therapy: from rainbow pills to polyagonists, Pharmacol. Rev. 70 (4) (2018) 712–746.
[55] B. Salehi, A. Ata, , V.A.K. N, F. Sharopov, K. Ramirez-Alarcon, A. Ruiz-Ortega, S. Abdulmajid Ayatollahi, P.V. Tsouh Fokou, F. Kobarfard, Z. Amiruddin Zakaria, M. Iriti, Y. Taheri, M. Martorell, A. Sureda, W.N. Setzer, A. Durazzo, M. Lucarini, A. Santini, R. Capasso, E.A. Ostrander, R. Atta ur, M.I. Choudhary, W.C. Cho, J. Sharifi-Rad, Antidiabetic potential of medicinal plants and their active components, Biomolecules 9 (10) (2019).
[56] D.W. Haslam, W.P. James, Obesity, Lancet 366 (9492) (2005) 1197–1209.